

BBA 42828

## The analysis of fluorescence induction transients from dichlorophenyldimethylurea-poisoned chloroplasts

John Sinclair and Sandra M. Spence

*Biology Department, Carleton University, Ottawa, Ontario (Canada)*

(Received 6 January 1988)

(Revised manuscript received 23 May 1988)

**Key words:** Chlorophyll fluorescence; Photosystem II; Dichlorophenyldimethylurea; Photosynthetic electron transport

A study has been done of the fluorescence induction curve from dichlorophenyldimethylurea (DCMU)-poisoned spinach chloroplasts and the area above this curve which represents the amount of oxidized electron acceptors available to Photosystem II. Analysis of the reduction of these electron acceptors unexpectedly suggested that the early kinetics of this process were dependent on whether the experiment was of short or long duration. Analysis of a theoretical fluorescence curve composed of the sum of two exponentials led to similar results and revealed that such misleading conclusions could be drawn from experiments if even small underestimates in the value of the final fluorescence level were made. It was shown that estimates of the rate constants of the exponentials were especially prone to error. A surprising result produced by the analysis of the theoretical results was the curved shape of the logarithmic plot of the area above the faster exponential. This was similar to the curves which have been found in the corresponding plots with chloroplast data and which have been given as evidence of exciton movement between photosystem II units. It was concluded that long illumination times improved the accuracy of these experiments. Analysis of the chloroplast data obtained from long-term experiments in this study suggested that there were not two, but three exponential phases present in the induction curves and that these phases persisted despite the presence of 5 mM hydroxylamine. The fluorescence induction curve from broken chloroplasts inhibited with DCMU was sensitive to the illumination conditions experienced by the organelles prior to the addition of DCMU. After 30 min of  $6 \mu\text{E} \cdot \text{m}^{-2} \cdot \text{s}^{-1}$  of 650 nm illumination, the final fluorescence level was 10% lower than that for the dark control. The area above the fluorescence induction curve was approx. 20% larger following light incubation and most of this increase could be attributed to a change in the slowest phase. It was suggested that pigment redistribution might be involved in this process.

Abbreviations: DCMU, 3-(3',4'-dichlorophenyl)-1,1'-dimethylurea; EDTA, ethylenediaminetetraacetic acid; CAD, complementary area decrease; Mops, 4-morpholinopropanesulfonic acid; PS I, Photosystem I; PS II, Photosystem II; HES, high-energy state.

Correspondence: J. Sinclair, Biology Department, Carleton University, Ottawa, K1S 5B6, Ontario, Canada.

### Introduction

The interpretation of the variable fluorescence induction kinetics from DCMU-poisoned, dark-adapted chloroplasts is based on the early work described in Refs. 1–4 and involves the area between the fluorescence curve and a line parallel to the time axis at an ordinate value equal to that of

the maximum level of fluorescence. This area is considered to be proportional to the number of electron acceptor molecules available for reduction by Photosystem II in DCMU-poisoned chloroplasts. At the start of illumination of dark-adapted chloroplasts, all of these acceptors are assumed to be in an oxidized state and as the variable fluorescence increases with time, the area above the curve lying to the left represents the amount of reduced acceptors and the area to the right represents the acceptors still in an oxidized state. The way in which these two areas change with time is complex and a number of hypotheses have been advanced to explain this complexity, examples of which can be found in Refs. 5–8. An important objective of this paper is not to add to this group of hypotheses, but rather to consider the analysis of the area changes above the fluorescence curve in some detail and ascertain what information can reasonably be derived from this type of analysis. In addition we report on the effect of the conditions of illumination prior to the start of a fluorescence induction experiment and how they influence the results.

## Methods

Chloroplasts for this study were isolated from 4-week-old, greenhouse-grown spinach. For relatively intact organelles, the isolation method used was Heber's modification [9] of the Jensen-Bassham procedure [10]. The proportion of chloroplasts with intact, outer membranes was routinely estimated with the ferricyanide method [11] and was found to be between 65% and 80%. Broken chloroplasts were prepared by suspending chloroplasts in a hypotonic medium containing 90 mM NaCl, 1 mM  $MgCl_2$  and 30 mM Mops (pH 7.8) for 3 min before centrifugation at  $2000 \times g$  for 90 s. The pellet was resuspended in 0.33 M sorbitol, 30 mM Mops (pH 7.8) and 1 mM  $MgCl_2$ . The chlorophyll concentration was measured using the procedure described in Ref. 12.

The fluorescence induction kinetics were observed with relatively intact chloroplasts suspended in the original Jensen-Bassham C medium [10] modified by the exclusion of sodium pyrophosphate and sodium isoascorbate and by the inclusion of 10 mM magnesium chloride. The

medium used with broken chloroplasts contained 0.33 M sorbitol, 30 mM Mops (pH 7.8), 10 mM  $MgCl_2$ , 50 mM NaCl and 0.1 mM methyl viologen. The chlorophyll concentration used was  $8 \mu g \cdot ml^{-1}$ . At the start of each experiment, the chloroplast suspension was dark-adapted for 5 min, then 100  $\mu l$  of a solution of DCMU (DuPont de Nemours & Co.) in ethanol was added in the dark to give a final DCMU concentration of 50  $\mu M$  (for most experiments). There was then another dark period of 1 min before the onset of illumination. In some experiments, the protocol just described was preceded by a preincubation period lasting for 30 min, during which time the chloroplasts were either kept in the dark or illuminated with light from a 300 W floodlamp (Westinghouse) filtered by 7 cm of water and an interference filter (peak transmission 650 nm, Baird Atomic, type B1) at an intensity of  $6 \mu E \cdot m^{-2} \cdot s^{-1}$ .

The chloroplast suspension was contained in a clear quartz cuvette and illuminated on all four sides by light-emitting photodiodes (Hewlett Packard, HLMP 3750). The wavelength of maximum emission of the photodiodes was 635 nm and the intensity used was  $12 \mu E \cdot m^{-2} \cdot s^{-1}$ . The power supply for the photodiodes was custom-built (Science Technology Centre, Carleton University) and produced a square-wave current modulated at the chosen frequency of 20 kHz. When the power was first switched on, the rise time of light emission was in the microsecond range and so a light shutter was unnecessary. The fluorescence emitted by the chloroplasts was observed through the base of the cuvette with a fibre-optics light guide and a photomultiplier tube (EMI, type 9659B) protected by a 690 nm interference filter. The output of the photomultiplier tube was measured with a lock-in amplifier (ITHACO, model 3962) whose time constant was set at 1 ms which determined the overall response time of the measurement system. The signal from the lock-in amplifier was digitized by an A/D board (Data Translation, DT2801) and then stored and processed in a microcomputer (Raven/8, Science Technology Centre, Carleton University). The software package used for signal processing was the Asyst software (Macmillan Software Co., version 1.56). A full-scale signal could be measured with 12 bit resolution.

After the fluorescence induction curve was recorded, a value of the maximum fluorescence ( $F_{\max}$ ) was determined as the mean value of the fluorescence during the final 10% of the illumination period. The initial value of the fluorescence ( $F_0$ ) was the value attained after three time constants or 3 ms of illumination. The area contained between  $F_{\max}$  and the fluorescence curve and between a time of 3 ms and any later time was determined by numerical integration and normalized with respect to the total area. In what follows, such an area is referred to as AREA normal, and in the Results section we have plotted the natural logarithm of  $(1 - \text{Area normal})$  as a function of time to evaluate rate constants. The latter will be termed a complementary area-decrease plot or a CAD plot. As explained above, a CAD plot describes the reduction of oxidized electron acceptors to Photosystem II. All CAD curves were analyzed as the sums of exponentials where this seemed appropriate, and the rate constants and amplitudes of these exponentials were determined from the straight lines giving the best least-squares fit of the data.

The earlier experiments in this work were performed with apparatus which permitted only the final values of the fluorescence to be measured with accuracy. In this situation, the chloroplasts were illuminated through one wall of the quartz cuvette with light which had been filtered through a blue glass long-wave cut-off filter (cut-off wavelength 550 nm). Fluorescence was observed perpendicular to the activating light with an optic light-guide and a photomultiplier tube shielded with a 690 nm interference filter (Baird Atomic, type B1). The activating light was intensity-modulated at 100 Hz and so the output of the photomultiplier tube was measured with a lock-in amplifier (Princeton Applied Research, type HR 8) connected to a chart recorder (Kipp and Zonen, type BD41) or a storage oscilloscope (Tektronix, type R5103N).

## Results

### *The analysis of fluorescence induction curves*

Three experiments were performed to observe the fluorescence induction transients from identical samples of suspended chloroplasts. These ex-

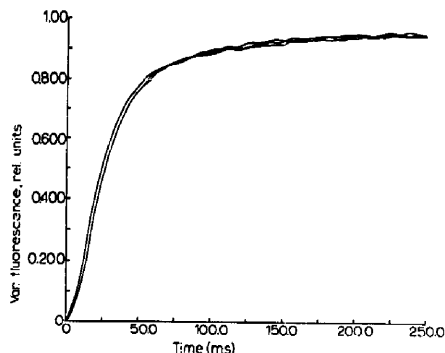


Fig. 1. The rise of the variable fluorescence signal from isolated chloroplasts in the presence of 50  $\mu\text{M}$  DCMU. These are the results for three experiments which were identical except for the duration of the illumination. The results were normalized with respect to the value of  $F_{\max}$  for each experiment. Other experimental conditions are described under Methods.

periments differed from each other only in the duration of the light period which was 2.5 s, 5.0 s and 10 s for the three experiments. As might be expected the initial kinetics were essentially the same for the three experiments (see Fig. 1). However the CAD curves derived from these three experiments showed very significant variations (Fig. 2). All three traces show an initial fast decline followed by an approximately linear decrease and a final period of accelerated decline. Clearly, the main differences between the three traces are the slopes and durations of the middle phases which decreased in slope and increased in duration as the illumination time was extended. Since

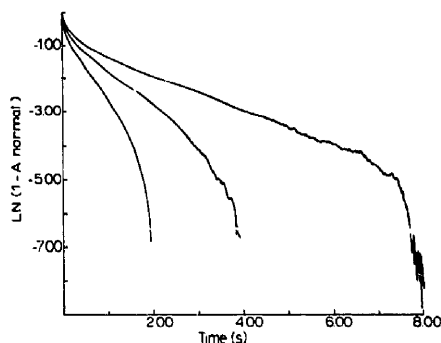


Fig. 2. Logarithmic plots of the complementary area decrease for the three experiments shown in Fig. 1.

we believed the physical processes underlying these curves to be identical in the three experiments, we concluded that at least two of the three curves must be significantly in error.

It seemed probable that the data analysis caused these errors and to investigate this idea we generated a theoretical set of results and treated them with the same method of analysis to see how accurate the results of our analysis were. Since CAD curves are often analyzed as the sum of two phases, of which one and sometimes two are thought to be exponential, we generated a theoretical fluorescence-induction curve as the sum of two exponential phases. This is shown in Fig. 3 where curves (2) and (3) are the fast and slow phases and curve (1) is their sum. Two CAD curves are shown in Fig. 4. Curve (1) was obtained using the mean value of 'fluorescence' between 950 and 1000 units of time as  $F_{\max}$  and while curve (2) used the mean of 'fluorescence' between 500 and 550 units of time as  $F_{\max}$ . The differences between these two curves are very similar to the differences between the curves in Fig. 2 and, thus, agree with our hypothesis that the method of data analysis can lead to false conclusions. The rapid decline seen at the end of both curves is due to concluding the analysis of data at a finite time, instead of at infinity as an exponential requires. This leads to two errors, (a) neglecting an area above the curve which should be included in the calculation and (b) assuming a final value for the fluorescence which is too low. These errors have particularly large effects as the value of the 'fluorescence' approaches the value of  $F_{\max}$ . We chose our theoretical curves so that our slow phase should have a slope of  $-0.003$  and our fast phase a slope of  $-0.03$  and each should contribute 50% to the area above the 'fluorescence' curve. The correct final value of the 'fluorescence' was 3.3. The values of  $F_{\max}$  were 3.28 for curve (1) ( $t = 1000$  time units) and 3.24 for curve (2) ( $t = 550$  time units), which were thus in error by 0.6% and 1.8%, respectively. The slopes of the middle phases of the two curves were estimated from what appeared to be the most linear regions and we obtained slopes of  $-0.00426$  (curve (1)) and  $-0.00787$  (curve (2)) so that the errors were 42% and 162%, respectively. However, when these results were used to estimate the areas associated

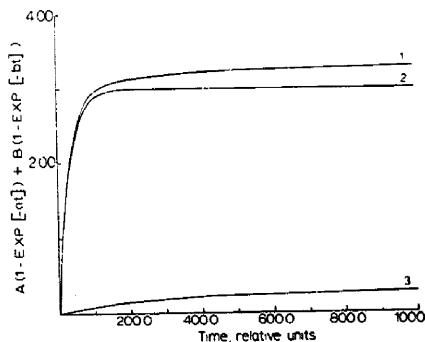


Fig. 3. Three exponential curves used to test the data analysis procedures. Curve (2) is an exponential whose rate constant is 0.03 and whose amplitude is 3.0 while curve (1) is an exponential whose rate constant is 0.003 and whose amplitude is 0.3. Curve (1) is the sum of these two curves and is the theoretical 'fluorescence' curve used in the test.

with the two phases, the calculated contributions of the slow phase were 49.6% (curve (1)) and 47% (curve (2)), which are quite close to the correct value. To complete the analysis, we subtracted the effect of the computed slow phases and plotted the surviving fast phases in Fig. 5, where it can be seen that neither of the traces are linear. While the average slope of curve (1) is  $-0.04$  and that of curve (2) is  $-0.0455$ , the corresponding average slopes for the first 50 points are  $-0.0327$  and  $-0.0358$ , which are much closer to the correct

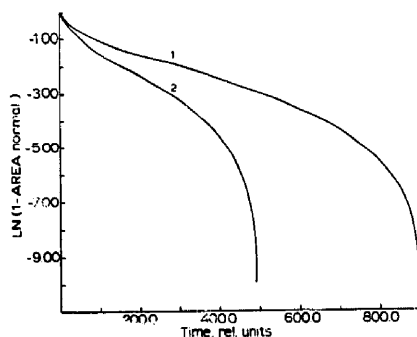


Fig. 4. Logarithmic plots of two complementary area-decrease curves derived from curve (1) in Fig. 3. The upper curve was calculated using a value of  $F_{\max}$  which was the mean of the last 50 points in curve (1), Fig. 3, while the lower curve used the points between 500 and 550. The complementary areas were calculated in the same way as those in Fig. 2.

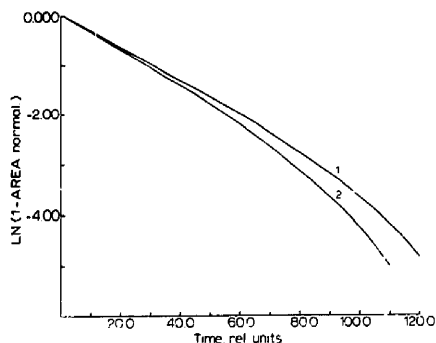


Fig. 5. Logarithmic plots of two complementary area-decrease curves derived from the corresponding curves in Fig. 4. The slopes and intercepts of the most linear sections of the two plots in Fig. 4 were each used to characterize the slow phase of curve (2) in Fig. 3. The influence of each slow phase was then eliminated from curve (1) in Fig. 3 and the new complementary area data were calculated for the two curves shown here.

value ( $-0.03$ ). We have thus demonstrated that this method of analysis can give reasonably good estimates of the relative contributions of the fast and slow phases to the areas above the fluorescence curve, even with short illumination times, but that the values of the slopes, especially the slower slope, are likely to be over-estimated to a significant extent unless the period of illumination is long compared with the time constant of the slow phase.

In Fig. 6 the results of an experiment are displayed in which fluorescence induction was observed in the presence of 5 mM hydroxylamine and 50  $\mu$ M DCMU. In comparison with the longest experiment in Fig. 2, we waited twice as long to assign a value to  $F_{\max}$  (18 s). The slope of the linear part of this trace is  $-0.25 \text{ s}^{-1}$  and the intercept which the extrapolation of this line makes with the ordinate corresponds to 39% of the total area above the fluorescence-induction curve. After subtracting the influence of this slowest phase from the fluorescence-induction curve, we generated the new CAD curve shown in Fig. 7, and this curve is also biphasic. The slope of the linear part of the curve is  $-1.3 \text{ s}^{-1}$  and the Y intercept corresponds to 28% of the total area above the fluorescence curve. Eliminating the influence of this phase in addition to the first, leads to a new CAD curve which is shown in Fig. 8. This is

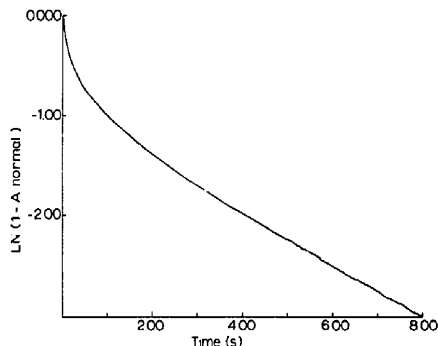


Fig. 6. Logarithmic plot of the complementary area decrease for an experiment in which a sample of chloroplasts was inhibited with 50  $\mu$ M DCMU and 5 mM hydroxylamine prior to the observation of fluorescence. The other experimental conditions were as described under Methods.

clearly a linear phase as well, with a slope of  $-9.0 \text{ s}^{-1}$ , and this phase accounts for the remaining 33% of the total area. As determined by regression analysis of variance, the total goodness of fit parameter for each of the best-fitting straight lines used above had a value of greater than 0.99 and was highly significant. The best-fitting straight lines used to describe the other CAD plots presented in this paper all yielded values of the

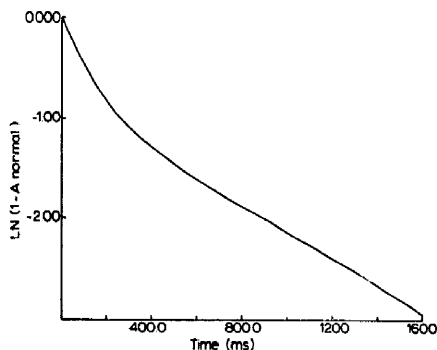


Fig. 7. Logarithmic plot of complementary area decrease derived from the corresponding curve in Fig. 6 by eliminating the influence of the slow phase seen in Fig. 6 from the fluorescence-induction curve and computing the complementary areas above the adjusted fluorescence curve. The procedures used were as described in Fig. 5. Note the biphasic nature of these two lines.

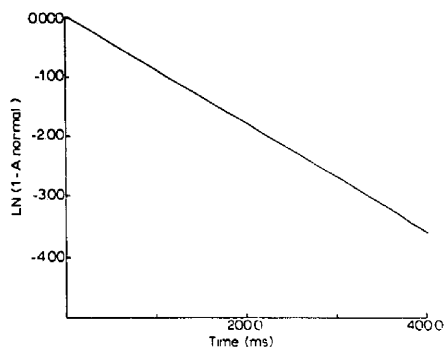


Fig. 8. Logarithmic plot of the complementary area decrease derived from the curve shown in Fig. 7 using a procedure similar to that described in the legend to Fig. 7.

goodness of fit parameter in excess of 0.99 and were very significant.

The linear traces used to describe the CAD plot in Fig. 6 tell us that we are dealing with three exponential processes. A similar description was obtained for the longest experiment shown in Fig. 2, but the rate constants were  $-0.5 \text{ s}^{-1}$ ,  $-3.2 \text{ s}^{-1}$  and  $-18.7 \text{ s}^{-1}$ , which are much higher. However, the areas associated with these three phases were 41%, 25% and 33%, which are very similar to those found above.

In what follows we shall refer to these three phases as the  $\alpha$ ,  $\beta$  and  $\gamma$  phases going from the fastest to the slowest phases in the CAD curve.

#### *The effect of prior illumination conditions on fluorescence-induction curves*

In the experiments described below, the chloroplasts were exposed to light or darkness for 30 min prior to the addition of DCMU and the observation of the fluorescence-induction curve. A comparison of the final fluorescence levels attained by broken chloroplasts inhibited by DCMU revealed that the effect of light incubation was to quench fluorescence emission by between 5% and 20% of the fluorescence emitted by dark-incubated organelles. The amount of fluorescence quenching due to light incubation varied with the particular chloroplast preparation. In a typical experiment, the level following dark incubation was  $100(\pm 5)\%$  and that following light incubation was  $86(\pm 6)\%$ , where the mean dark value has been set at 100%

and the figure in brackets is the standard deviation. When this experiment was repeated in the presence of 5 mM  $\text{NH}_4\text{Cl}$ , the corresponding figures were  $99(\pm 4)\%$  (dark) and  $74(\pm 7)\%$ , revealing that the final fluorescence level was quenched after light incubation even in the presence of an uncoupler of photophosphorylation. The final fluorescence level from light-incubated chloroplasts was not significantly different from that from dark-incubated chloroplasts if DCMU was omitted ( $99(\pm 4)\%$  versus  $100(\pm 6)\%$ ). When intact chloroplasts were examined, the results were very similar to those with broken chloroplasts. The value for light-incubated chloroplasts in the presence of DCMU was  $88(\pm 6)\%$  compared with  $100(\pm 6)\%$  for the dark-treated organelles. Both the incubation time and the intensity of light during incubation had significant effects on the quenching of fluorescence in the light. For example, in an experiment in which a 30 min light incubation caused a quenching of 6%, doubling the incubation time increased this to 11%. Also, in an experiment where 30 min of light incubation at the usual light intensity caused a quenching of 8%, doubling the intensity produced a quenching of 17%.

To explore the effects of light and dark incubation in more detail, we investigated the fluorescence-induction curve, two examples of which are shown in Fig. 9. We normalized both of these curves with respect to the mean value of fluorescence found between 18 s and 20 s, and we also subjected them to a curve-smoothing procedure. These two experiments were performed with intact chloroplasts and the fluorescence was observed in the presence of 5 mM  $\text{NH}_4\text{OH}$  and 50  $\mu\text{M}$  DCMU. Both curves have the usual sigmoidal shape, but the curve from the light-incubated sample rises more slowly than the other curve and reached only 92% of its final value after 1 s, compared with 95% for the curve for the dark-incubated sample. The maximum value of the variable fluorescence for the light-incubated sample was 11% less than the value for the dark-incubated sample. There was no significant difference in the values of  $F_0$  for these two experiments.

The complementary area decreases for these experiments were computed and are plotted as logarithmic functions of time in Fig. 10. Both of these traces exhibit an initial, fast decline followed

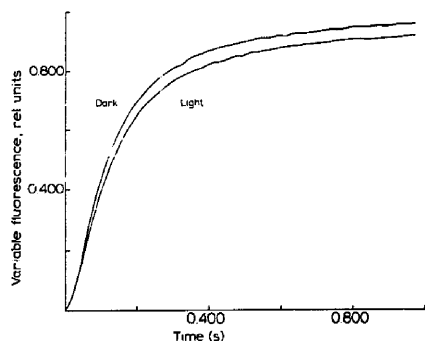


Fig. 9. Variable fluorescence as a function of time from two samples of chloroplasts, one of which had been exposed to light ( $650 \text{ nm}$ ,  $6 \mu\text{E} \cdot \text{M}^{-2} \cdot \text{s}^{-1}$ ) and one which had been kept in darkness for 30 min.  $5 \text{ mM}$  hydroxylamine and  $50 \mu\text{M}$  DCMU were present when fluorescence was observed. These results were subjected to a curve-smoothing procedure. Other experimental conditions are given in under Methods.

by slower, linear fall which indicates an exponential process. The slopes of these  $\gamma$  phases are very similar but the intercepts which their projections make with the ordinate are quite different.

Elimination of the  $\gamma$  phases from the fluorescence curves generated two new CAD curves describing only the fast, initial changes as shown in Fig. 11. These traces are quite similar but there appear to be small differences in the slopes and intercepts of the linear phases. We repeated the process of subtracting the influence of the slow,  $\beta$  phases and thus generated the final, two CAD

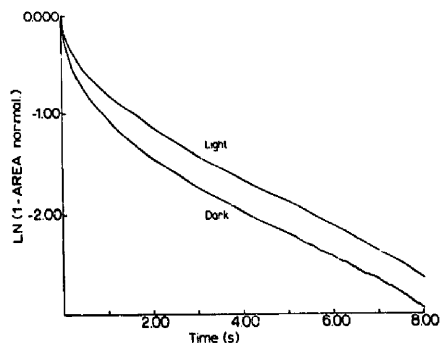


Fig. 10. The complementary area decreases for the experiments in Fig. 9 plotted logarithmically as a function of time.

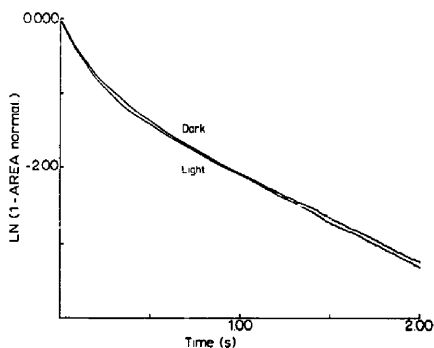


Fig. 11. The complementary area decreases derived by subtracting the influence of the slowest phase seen in Fig. 10 from the fluorescence curves in Fig. 9 and calculating the areas above the adjusted fluorescence curves.

curves shown in Fig. 12. These are the  $\alpha$  phases and to a good approximation these are straight lines with very similar slopes.

A numerical description of these two experiments along with another experiment in which intact chloroplasts were incubated in the light in the presence of the uncoupler  $\text{NH}_4\text{Cl}$  ( $5 \text{ mM}$ ) is presented in Table I. Each CAD curve has been analyzed as the sum of three exponentials and it can be seen that the rate constants for the different phases had very similar values in the three experiments. However, the relative sizes of the three areas associated with these phases are

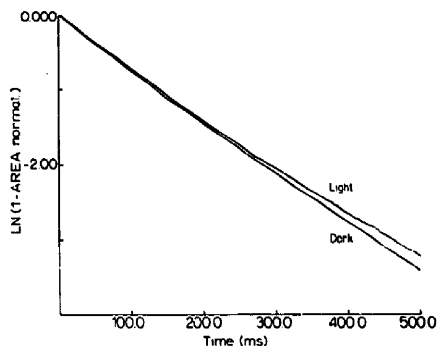


Fig. 12. The complementary area decreases corresponding to the initial fast phases in Fig. 11 plotted logarithmically as functions of time

TABLE I

## THE RATE CONSTANTS AND AREAS ASSOCIATED WITH THE THREE KINETIC PHASES OF FLUORESCENCE INDUCTION

The results are from two experiments shown in Fig. 9 and another light experiment performed in the presence of 5 mM  $\text{NH}_4\text{Cl}$ . Fluorescence was observed in the presence of 50  $\mu\text{M}$  DCMU and 5 mM hydroxylamine. The rate constants and areas are the slopes and intercepts of the best-fitting straight lines for the logarithmic CAD plots. The goodness of fit parameter was greater than 0.99 in every case as determined by regression analysis of variance.

Expt.	Rate constants ( $\text{s}^{-1}$ )			Areas (% of total area)			Areas (absolute values, relative units)			Total area (relative units)
	$\alpha$	$\beta$	$\gamma$	$\alpha$	$\beta$	$\gamma$	$\alpha$	$\beta$	$\gamma$	
Light	6.4	1.3	0.24	27	23	50	128	106	235	469
Dark	6.8	1.2	0.23	39	27	34	152	106	133	391
Light + $\text{NH}_4\text{Cl}$	7.0	1.4	0.23	25	21	54	128	110	280	518

markedly different with about 50% being associated with the  $\gamma$  phase in both the light-incubated samples and only 34% in the  $\gamma$  phase of the dark-incubated sample. Both the  $\alpha$  phase and the  $\beta$  phase are relatively larger in the dark-incubated sample. A somewhat changed picture appears when we consider the actual areas above these three curves. The total areas above the induction curves for the light-incubated samples are larger than that for the dark-incubated sample but they are also different from each other. The difference between the light-incubated samples can be entirely ascribed to the  $\gamma$  phases, since the  $\alpha$  and  $\beta$  phases are identical. In contrast the dark-incubated sample differs from the other two samples in that it has a smaller  $\gamma$  phase and a larger  $\alpha$  phase, while the area associated with the  $\beta$  phase remains almost constant in all three samples. The final value of the variable fluorescence for the chloroplasts incubated in the presence of the uncoupler and light was 11% less than the dark value.

### Discussion

Although fluorescence-induction transients have been observed and interpreted by many workers, surprisingly little attention has been given to the flaws which might be present in such experiments. Important exceptions to this are the

works of Bell and Hipkins [13] and Schreiber and Pfister [14] who both stressed the importance of using an adequately long period of illumination when performing fluorescence induction experiments. Bell and Hipkins [13] demonstrated this by treating the results of one of their experiments in the same manner as we did with our theoretical fluorescence curve and generated similar effects. A major advantage of using a theoretical curve to study the analysis procedure is that the correct values of the parameters are known and can be compared with the results of calculations and, hence, the reliability of the analysis ascertained. Thus, we have found that there will always be a final, very fast decline in the area growth curves which is due to the need to assume a finite time when the fluorescence has reached its final value. This assumption also affects the slope values obtained so that an error of as little as 0.6% in the estimate of the value of  $F_{\text{max}}$  can cause the slope of the slow phase to be over-estimated by 42%. It is therefore clear that attempts to measure the rate constants associated with fluorescence-induction curves are only likely to yield accurate information if extreme care is taken to estimate the  $F_{\text{max}}$  value accurately. In contrast, the division of area between the fast and slow components was not nearly so sensitive to the error in  $F_{\text{max}}$ . The reason for the change in slope of the slow phase in the two curves in Fig. 4 is associated with the position



of the linear regions. For curve (1) this lay at a later time than for curve (2) and there was thus less overlap between the two exponential phases which had been used to construct these data and, hence, a more accurate estimate of the slope was obtained. It seems very probable that a similar explanation applies to the results shown in Fig. 2. The calculated fast phases were also significantly in error with respect to their slopes and form. However, the errors in the slopes were not too great (about 10%) if only the earlier parts of the curves were used for the calculation.

The most surprising result of these calculations was the curved appearance of these fast phases where a linear trace would have been the ideal result. Downwardly concave fast phases have been found by groups working with chloroplast preparations, for example Melis and Duysens [15] who interpreted these curves as evidence that there was excitation energy transfer interactions between Photosystem II units (see Fig. 7 [15]). We cannot say that the groups who have observed such curved fast phases with chloroplasts are wrong in their interpretations, but we do believe that a fresh look at all such claims is required, to rule out the possibility that the curvature is simply an artifact of the data analysis. With the longer periods of illumination used in this study we consistently obtained CAD curves which are best described as the sum of three exponentials.

Having demonstrated that the method of data analysis can cause errors, we must ask whether our experiments have yielded data which can be regarded as reliable. As the theoretical study demonstrated that the duration of the illumination period was of crucial importance in obtaining results which were accurate, we tried to extend our experiments until the results did not change any further. As was shown, this was not entirely successful, since the slopes of the phases decreased with longer periods of illumination and so we must regard the slope values we obtained as being too large. However, the areas above the fluorescence curves associated with the three phases did appear to be reproducible for the two longest illumination periods and can probably be accepted as reasonable estimates. This difference in the reliability of the two types of result is in accord with our theoretical findings.

A major result emerging from this study is the existence of three phases in the CAD plots. This is in contrast to results found by earlier workers (e.g., Ref. 15) who found only two phases which were described in the  $\alpha$  and  $\beta$  phases. We believe that the presence of this third and slowest phase has gone undetected because most earlier fluorescence-induction experiments were concluded too soon for this phase to become apparent. Examination of the results in Refs. 13 and 14 suggests that the  $\gamma$  phase was observed, but it was not recognized. Indeed, Schreiber and Pfister [14] discussed the slowest phase in their results as if it were the  $\beta$  phase, but they did not include an analysis of the initial part of their CAD curves in their paper and so did not have an opportunity to identify the  $\gamma$  phase. As mentioned earlier, a number of hypotheses have been advanced to explain the nature of the distinction between the  $\alpha$  and  $\beta$  phases. It now appears that these hypotheses will have to be re-examined because of the existence of this third phase. The nature of this third phase is unclear, but we can offer evidence that at least its existence does not depend, to any significant extent, on a cyclic back-flow of electrons around PS II. This is because the number of phases, their exponential nature and their relative sizes were unaffected by the presence of 5 mM hydroxylamine (compare the analysis of Fig. 6 and the longest experiment in Fig. 2).

Our discovery that the incubation of chloroplasts in the light causes a quenching of fluorescence is reminiscent of the photoquenching phenomenon reported previously [16]. The latter was shown to involve the formation of a hydrogen ion gradient across the thylakoid membrane or high-energy state (HES) and was found to occur in whole cells, intact chloroplasts and broken chloroplasts [17]. The circumstances which control the manifestation of HES-dependent fluorescence quenching in broken chloroplasts include (a) the presence of ascorbate or azide or NADP and ferredoxin; (b) the absence of uncouplers of photophosphorylation; and (c) the absence of DCMU at concentrations in the micromolar range or higher. Thus, we can be confident that HES-dependent fluorescence quenching was not involved here, since the effect we found was in the presence of 20  $\mu$ M DCMU and with chloroplasts which

were uncoupled during light exposure. In the case of intact chloroplasts, it might be thought that the quenching was due to a redistribution of more absorbed light energy towards PS I as a result of the phosphorylation of the thylakoid membrane proteins. However, the incubation of such chloroplasts in the presence of light and  $\text{NH}_4\text{Cl}$  still produced the fluorescence quenching. Another possible explanation for this quenching could be a light-stimulated leakage of electrons from the reducing side of PS II to the oxidizing side. To explore this possibility we injected 5 mM  $\text{NH}_2\text{OH}$  into the bathing medium along with the DCMU, since this is believed to prevent this leakage of electrons by reducing the redox compounds on the oxidizing side of PS II [18]. The presence of  $\text{NH}_2\text{OH}$  did not prevent the light-induced quenching of fluorescence and so this idea does not appear to be valid. We conclude that the fluorescence quenching found here cannot be readily explained by any of the currently accepted mechanisms and a new mechanism is required.

The light-induced fluorescence quenching seen in this study is associated with changes in the total area above the fluorescence-induction curve (Table I). As explained above, the area above the fluorescence-induction curve is related to the total number of electron acceptors available to PS II before the site of inhibition by DCMU. However, such a straightforward interpretation must be qualified, since there are different kinetic phases present as fluorescence induction develops [19] and, as has been pointed out [20], it is possible that the quantum efficiency of fluorescence emission may be different for each of these kinetic phases. Thus, the total number of electron acceptors would depend on the relative amounts of the different phases which were present and not merely on the total area above the fluorescence curve. Hence, when we examine Table I and see that the total area above the fluorescence-induction curve was smaller after dark incubation, we cannot say that this is conclusive evidence of a decrease in the number of electron acceptors without some knowledge of the quantum efficiencies of the three phases. All that can be stated is that there was a decrease in the amount of the  $\gamma$  phase and an increase in the amount of the  $\alpha$  phase.

Many papers dealing with CAD curves have

made comparisons on the basis of the percentage areas occupied by the  $\alpha$  and  $\beta$  phases in the experiments that have been compared (e.g., Refs. 14, 21 and 22). As we have shown in Table I this type of comparison can lead to a significantly different description of events from one based on absolute area determinations. To be specific, our percentage area figures suggest that the  $\beta$  phase is significantly larger following dark incubation, while our absolute area results suggest that the  $\beta$  phase is unchanged in all three experiments. Hence, a description based solely upon relative areas can lead to a serious misunderstanding of events when there are large differences in the total areas above the curves, and we suggest that future studies involving comparisons of the areas above fluorescence curves should include estimates of the total areas.

All the leaves employed for the isolation of chloroplasts in this work had been kept in the dark for a minimum of 2 h prior to their use. There was a brief exposure to room light (about 5 min) during chloroplast isolation and then the chloroplasts were kept in the dark until the experiments were performed. We consider that prior to light incubation all the chloroplasts were in a dark-adapted state. Starting from this assumption, we propose the following model as a possible explanation for these results and as a basis for further work. The  $\alpha$ -phase represents a group of PS II reaction centres, each of which are associated with a large number of pigment molecules. Once light incubation begins, there is a dissociation of some of the pigment molecules (which are probably bound to proteins) from these  $\alpha$  PS II centres, leaving behind smaller complexes which we detect as the increase in the number of centres in the  $\gamma$  phase. The pigment molecules which become dissociated could become associated with PS I complexes or with new PS II reaction centres which are activated by the light. This would leave the  $\beta$  phase as an unchanging group of PS II centres possibly located in the non-appressed regions of the thylakoid membranes as has been suggested [23]. The decline in fluorescence could occur as a result of the transfer of pigment molecules to PS I or because of a decreased quantum yield in  $\gamma$  centres compared with  $\alpha$  centres. The slow kinetics of the  $\gamma$  phase would appear because

of the smaller light-harvesting capabilities of the smaller number of pigment molecules per reaction centre.

### Acknowledgements

This work was supported by grants from the Natural Sciences and Engineering Research Council of Canada and Carleton University. DCMU was a gift from E.I. du Pont de Nemours and Co. Thanks are due to Dr. P. Heytler and Ms. J.L. Singleton for their help. The skilled assistance of Mr. L. Speers, Biology Department, Carleton University with the preparation of this paper is gratefully acknowledged.

### References

- 1 Duysens, L.N.M. and Sweers, H.E. (1963) in *Microalgae and Photosynthetic Bacteria* (Japanese Society for Plant Physiology), pp. 353–372, University of Tokyo Press, Tokyo.
- 2 Bennoun, P. and Li, Y.S. (1973) *Biochim. Biophys. Acta* 292, 162–168.
- 3 Murata, N., Nishimura, M. and Takamiya, A. (1966) *Biochim. Biophys. Acta* 120, 23–33.
- 4 Malkin, S. and Kok, B. (1966) *Biochim. Biophys. Acta* 126, 413–432.
- 5 Bulychiev, A.A. and Gyenes, M. (1985) *Biophysics* 30, 263–285.
- 6 Melis, A. and Homann, P.H. (1975) *Photochem. Photobiol.* 21, 431–437.
- 7 Morin, P. (1964) *J. Chem. Phys.* 61, 674–680.
- 8 Joliot, A. and Joliot, P. (1964) *C.R. Acad. Sci. Paris Ser. D* 250, 4622–4625.
- 9 Heber, U. (1973) *Biochim. Biophys. Acta* 305, 140–152.
- 10 Jensen, R.G. and Bassham, J.A. (1966) *Proc. Natl. Acad. Sci. USA* 56, 1095–1098.
- 11 Heber, U. and Santarius, K.A. (1972) *Naturforsch.* 25b, 718–728.
- 12 Vernon, L.P. (1960) *Anal. Chem.* 32, 1144–1150.
- 13 Bell, D.H. and Hipkins, M.F. (1985) *Biochim. Biophys. Acta* 807, 255–262.
- 14 Schreiber, U. and Pfister, K. (1982) *Biochim. Biophys. Acta* 680, 60–68.
- 15 Melis, A. and Duysens, L.N.M. (1979) *Photochem. Photobiol.* 29, 373–382.
- 16 Krause, G.H. (1974) *Biochim. Biophys. Acta* 333, 301–303.
- 17 Briantais, J.-M., Verrotte, C., Picaud, M. and Krause, G.H. (1979) *Biochim. Biophys. Acta* 548, 128–138.
- 18 Homann, P.H. (1971) *Biochim. Biophys. Acta* 245, 129–143.
- 19 Melis, A. and Homann, P.H. (1978) *Arch. Biochem. Biophys.* 190, 523–530.
- 20 Joliot, P., Bennoun, P. and Joliot, A. (1973) *Biochim. Biophys. Acta* 305, 317–328.
- 21 Kyle, D.J., Haworth, P. and Arntzen, C.J. (1982) *Biochim. Biophys. Acta* 680, 336–342.
- 22 Sundby, C., Melis, A., Mäenpää, P. and Andersson, B. (1986) *Biochim. Biophys. Acta* 881, 478–483.
- 23 Andersson, J.M. and Melis, A. (1983) *Proc. Natl. Acad. Sci. USA* 80, 745–749.